

AR-010-621

19981112 032

Analysis of the Interaction Effect for  
Bonded Repairs

R.J. Callinan, L.R.F. Rose and  
S. Sanderson

DSTO-TR-0715

APPROVED FOR PUBLIC RELEASE

© Commonwealth of Australia

# Analysis of the Interaction Effect for Bonded Repairs

*R.J. Callinan, L.R.F. Rose and S. Sanderson*

**Airframes and Engines Division  
Aeronautical and Maritime Research Laboratory**

DSTO-TR-0715

## ABSTRACT

With the increasing use of bonded repairs to restore the structural integrity of ageing aircraft the question arises as to the interaction effects when repairs are located close together. Using the Finite Element (F.E.) method a study has been carried out for the interaction between two idealised circular repairs. The interaction involves the increase of the sheet stress just outside the patch. It has been found that the tandem orientation, with respect to the applied load, is the most severe configuration. In this case, for most practical repairs, the interaction may result in increases of the sheet stress by 40% for very close separation distances. It has also been found that certain combinations of bi-axial load can also significantly influence the interaction effect.

## RELEASE LIMITATION

*Approved for public release*

DEPARTMENT OF DEFENCE

DEFENCE SCIENCE AND TECHNOLOGY ORGANISATION

*Published by*

*DSTO Aeronautical and Maritime Research Laboratory  
PO Box 4331  
Melbourne Victoria 3001*

*Telephone: (03) 9626 7000  
Fax: (03) 9626 7999  
© Commonwealth of Australia 1998  
AR-010-621  
August 1998*

**APPROVED FOR PUBLIC RELEASE**

# Analysis of the Interaction Effect for Bonded Repairs

## Executive Summary

The repair of cracked structures using bonded repairs has resulted in considerable aircraft lifetime extension and hence cost savings. The long fatigue life of a bonded repair is attributed to the lack of rivets and hence stress concentrations in the repair. However the widespread use of these repairs for ageing aircraft may result in repairs being located close together. The purpose of this study is to determine the factors that influence the sheet stress just outside the patch.

The finite element method is used to analyse the problem, and for convenience the reinforcement has been modelled to be a circular patch with constant thickness. The first geometric configuration considered is the tandem configuration with respect to the applied load. This is the most severe configuration and for most practical repairs, the interaction may result in increases of the sheet stress by 40% for very close separation distances. It has also been found that certain combinations of bi-axial applied load can also significantly influence the interaction effect. In the case of a periodic array of repairs in the tandem configuration under a uni-axial load the highest sheet stresses are increased by 60% for close separations. In the case of the side-by-side configuration the sheet stresses are increased only by 19% for most practical repairs, and correspond to large separation distances. A finite width effect has been investigated for the tandem configuration and it has been found that for small widths the sheet stress is lowered by as much as 13%. For all configurations considered over stiff repairs gave the maximum stress increases.

The design of bonded repair procedures is well documented in the RAAF Engineering Standard, C5033. However the current load attraction factor used for bonded repairs does not take account of the separation distance between repairs. The purpose of the work presented here is to present design curves which, when used together with material S-n data, will enable the RAAF to more accurately assess the fatigue life of the sheet just outside repairs.

## Authors

### **R.J. Callinan**

Airframes and Engines Division

*Mr. R.J. Callinan is a senior research scientist and graduated from RMIT (Aero. Eng.) in 1969 and from Monash University in 1971 (Civil. Eng.) and completed a M.Eng. Sc. in 1981 at Melbourne University. His work has been in the areas of finite element analysis, fracture mechanics and structural mechanics of composite and bonded repairs, and military aircraft accident investigations. He has also been involved with design studies of low radar cross-section battlefield surveillance R.P.V.'s. In 1985 he was seconded to the USAF at Eglin AFB for 18 months, to carry out vulnerability studies on composite structures.*

---

### **L.R.F. Rose**

Airframes and Engines Division

*Francis Rose graduated with a B.Sc (Hons) from Sydney University in 1971 and a PhD from Sheffield University, UK in 1975. He was appointed as a Research Scientist at the Aeronautical Research Laboratory in 1976 and is currently the Research Leader in Fracture Mechanics in the Airframes and Engines Division.*

*He has made important research contributions in fracture mechanics, non-destructive evaluation and applied mathematics. He is the regional Editor for the International Journal of Fracture and a member of the editorial board of Mechanics of Materials. He is also a Fellow of the Institute for Applied Mathematics and its Applications, UK and a Fellow of the Institution of Engineers, Australia.*

---

### **S. Sanderson**

Airframes and Engines Division

*Mr. Sanderson has worked at AMRL since 1981. He has developed flight data reduction & analysis software for Mirage, F-111 & F/A-18 projects. Several of these programs have been implemented by NAE for part of their data reduction in the IFOSTP project. Since 1992, Mr. Sanderson has undertaken finite element analysis of composite and bonded structures for the F-111 and F/A-18 aircraft and provided training in finite element modelling and analysis.*

---

# Contents

1. INTRODUCTION.....	1
2. F.E. METHODOLOGY.....	1
3. RESULTS .....	3
3.1 Tandem configuration.....	3
3.2 Side by side configuration .....	5
3.3 Periodic array .....	6
3.4 Combination of loads .....	7
3.5 Finite width effect.....	8
4. VALIDATION .....	11
5. CONCLUSION .....	15
6. ACKNOWLEDGMENT .....	16
7. REFERENCES .....	17

## 1. Introduction

The repair of cracked aircraft structures using bonded repairs has resulted in considerable aircraft lifetime extension and hence cost savings. The long fatigue life of a bonded repair is attributed to the lack of rivets and hence stress concentrations in the repair. However the widespread use of these repairs for ageing aircraft may result in repairs located close together. The purpose of this study is to quantify the interaction effect. The existence of this effect has been shown in Chow and Atluri [1] for limited geometries. In the work carried out here, a parametric study is carried out. In this study the increase in the stress in the sheet just outside the patch is the quantity being considered. The orientation of the repairs is considered with respect to the applied load. Furthermore biaxial loadings will be considered. The finite width effect is also considered for two different configurations. The analysis is considered as linear elastic. The design of bonded repair procedures is well documented in the RAAF Engineering Standard, C5033 [2]. However the current load attraction factor used for bonded repairs does not take account of the separation distance between repairs. The purpose of the work here is to present design curves which, when used together with material S-n data, will enable the RAAF to more accurately assess the fatigue life of the sheet just outside repairs.

## 2. F.E. Methodology

The representation of the repair in this analysis is simplified and does not include the adhesive, in accordance with stage 1 of the two-stage design analysis proposed by Rose [3] for repair design. For convenience the reinforcement has been modelled to be a circular patch with constant thickness using a 2D linear elastic finite element analysis. Only in-plane loads are considered, and out-of-plane secondary bending has been restrained. Thus the analysis is most appropriate for two-sided repairs, or for cases where out-of-plane deflection is restrained by stiff sub-structure Rose et. al. [4]; one-sided repairs introduce geometrical non-linearity and new length-scales which are not considered here Wang et. al. [5]. Also it was assumed that the hole or crack being reinforced does not affect the load being drawn into the patch. As a result a simple model has been developed in which the variables are firstly the ratio of the combined Young's modulus of the patch and sheet beneath,  $E_o$ , to the sheet modulus,  $E_s$ , as indicated in Fig. 1, and secondly by the separation distance,  $2S$ , between the two repairs (Fig. 2). From equilibrium considerations the  $E_o / E_s$  ratio for any repair, as shown in Fig. 1, is given by:

$$\frac{E_o}{E_s} = \frac{E_s t_s + E_p t_p}{E_s t_s} \quad (1)$$

where

$E_p$  Young's modulus for the patch

$t_s$  thickness of the sheet  
 $t_p$  thickness of the patch

For most repairs  $E_p t_p = E_s t_s$ , hence  $E_o / E_s = 2$ . For an over-stiff repair  $E_p t_p > E_s t_s$ .

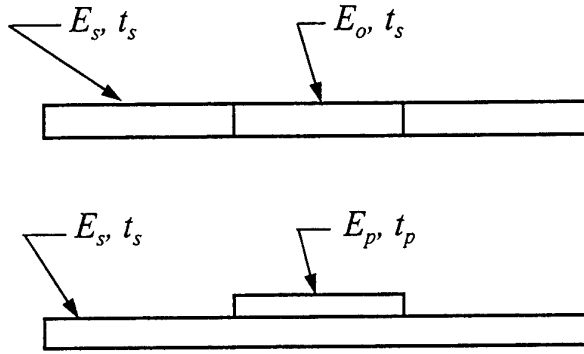


Figure 1. The geometry for an equivalent stiffness representation.

Load cases considered are for remote  $\sigma_x$  and  $\sigma_y$  stresses and a combination of both  $\sigma_x$  and  $\sigma_y$ . The axis system used is shown in Fig. 2.

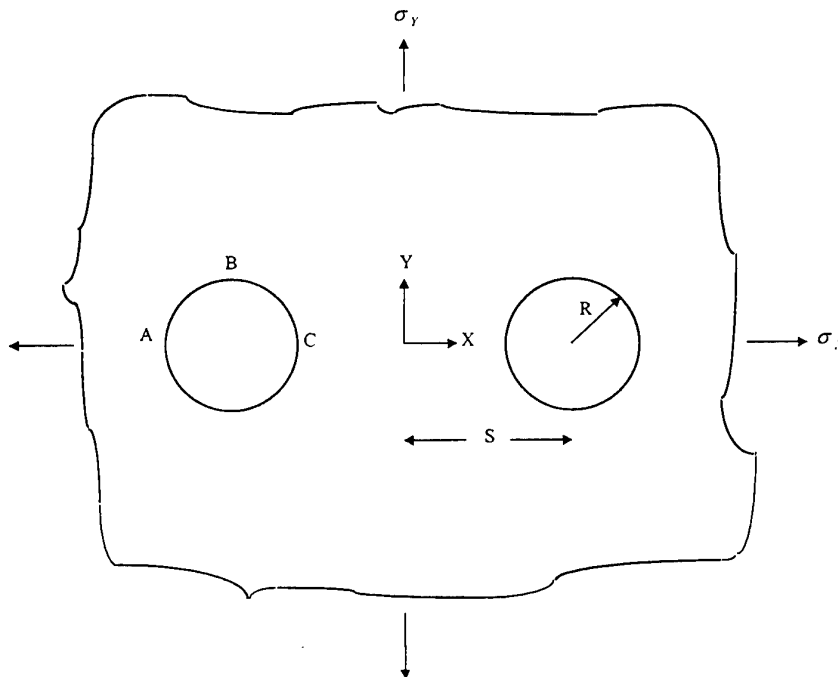


Figure 2. Two repairs in an infinite sheet: axis system and locations of interest.

The separation between the repairs is expressed as a ratio of  $S/R$ . Shown in Fig. 2 is a close up view of the F.E. mesh for a separation ratio of 1.1. A range of separation ratios of 1.1 to 5 will be considered.

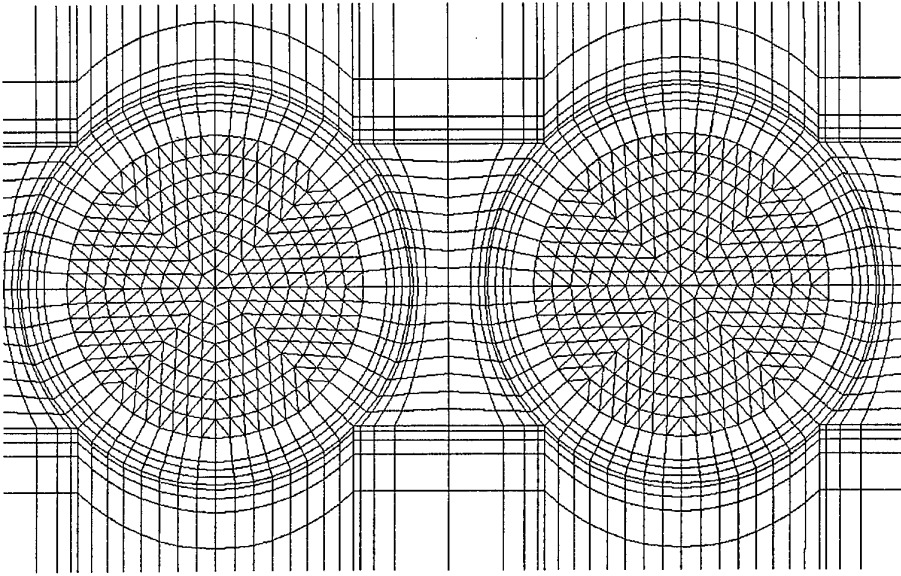


Figure 3. Close up view of mesh for  $S/R=1.1$

### 3. Results

This configuration is shown in Fig. 4 and corresponds to an applied stress of  $\sigma_x = 1$  and  $\sigma_y = 0$ . The stress contours indicate that the maximum principal stress,  $\sigma_1$ , occurs at location C (see Fig. 2). Also it happens that the maximum principal stress occurs in the X direction. The results for this configuration with respect to the applied load are shown in Fig. 5 and indicate a strong interaction for close separation and high  $E_o / E_s$  values, and maximum stress ratio of 1.60 was achieved. Normally a repair would correspond to  $E_o / E_s = 2$  and hence would correspond to a maximum stress ratio of 1.4. At large separation distances  $\sigma_1$  approaches an asymptotic value which corresponds to that of a single repair.

#### 3.1 Tandem configuration

This configuration is shown in Fig. 4 and corresponds to an applied stress of  $\sigma_x = 1$  and  $\sigma_y = 0$ . The stress contours indicate that the maximum principal stress,  $\sigma_1$ , occurs at location C (see Fig. 2), and this location is independent of the  $S/R$  ratio. Also it happens that the maximum principal stress occurs in the X direction. The results for

this configuration with respect to the applied load are shown in Fig. 5 and indicate a strong interaction for close separation and high  $E_o / E_s$  values, and maximum stress ratio of 1.60 was achieved. Normally a repair would correspond to  $E_o / E_s = 2$  and hence would correspond to a maximum stress ratio of 1.4. At large separation distances  $\sigma_1$  approaches an asymptotic value which corresponds to that of a single repair.

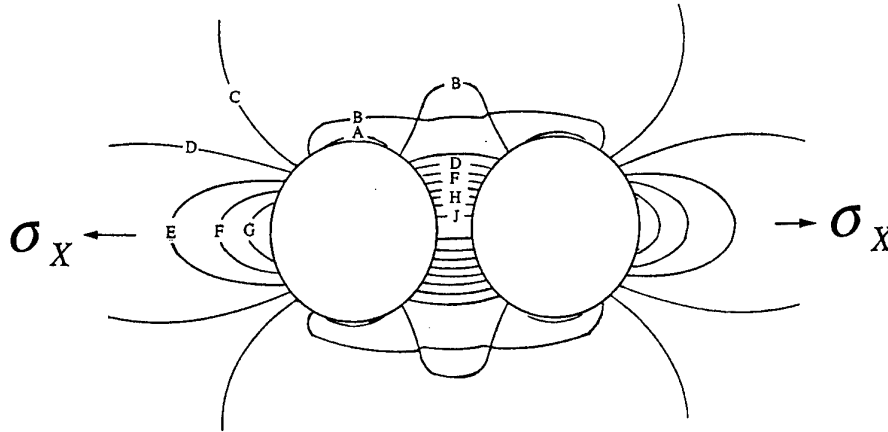


Figure 4. Tandem configuration: stress interaction between two circular repairs, where  $\sigma = \sigma_x = 1$  and  $S/R = 1.2$ . (A=.878, B=.928, C=.977, D=1.027, E=1.076, F=1.126, G=1.175, H=1.225, I=1.274, J=1.324)

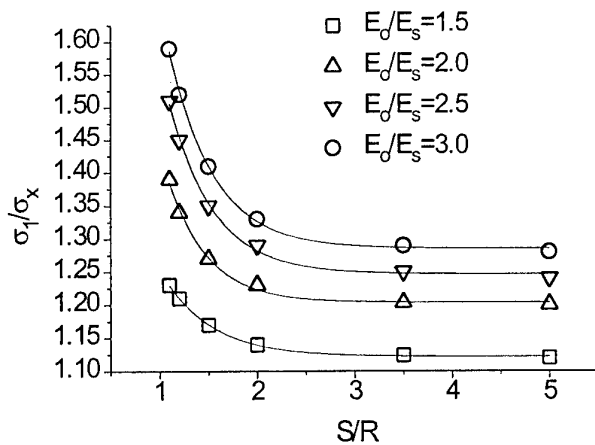


Figure 5. Tandem configuration: variation of stress ratio  $\sigma_1/\sigma_x$  with  $S/R$  ratio.

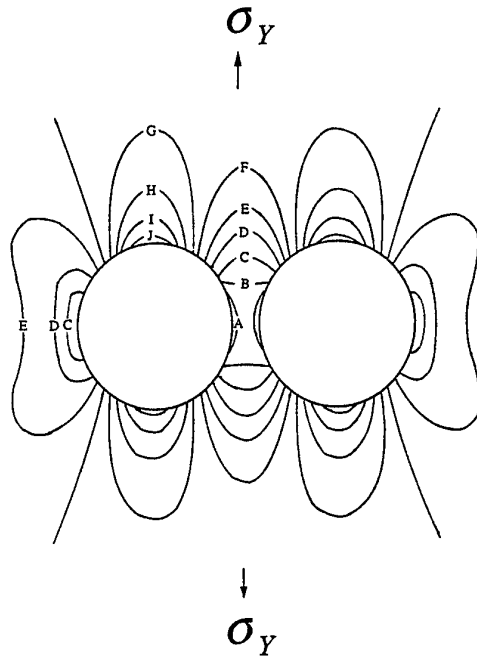


Figure 6. Side by side configuration: stress interaction between two circular repairs, where  $\sigma_x=1$ . and  $\sigma_y=0$ . and  $S/R=1.2$  (A=.810, B=.848, C=.886, D=.925, E=.963, F=1.001, G=1.039, H=1.078, I=1.116, J=1.154)

### 3.2 Side by side configuration

This configuration is shown in Fig. 6 and corresponds to the applied loading  $\sigma_x = 0$  and  $\sigma_y = 1$ . In this case the stress contours for the maximum principal stress show that the maximum value occurs at location B (see Fig. 2), and this location is independent of the S/R ratio. Also it happens that the maximum principal stress occurs in the Y direction. The results for a study of the interaction are shown in Fig. 7. These results are different to the previous case in that the maximum stress ratios occur at large separations, due to shielding, and show an asymptotic behaviour. As before, the maximum stress concentration in the sheet occurs for high  $E_o / E_s$  values. The maximum stress ratio achieved was 1.28. Again, for most repairs ( $E_o / E_s = 2.$ ) and the maximum stress ratio is 1.19.

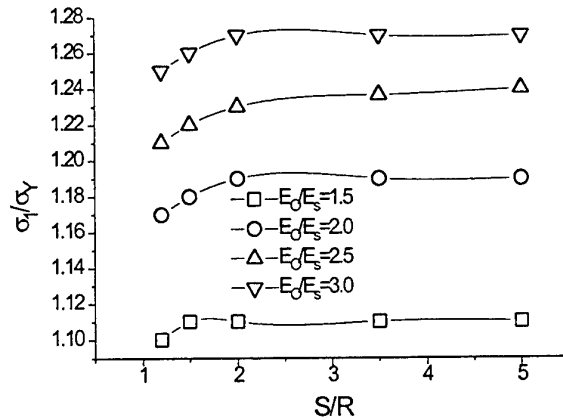


Figure 7. Side by side configuration: variation of stress ratio  $\sigma_1 / \sigma_y$  with  $S/R$  ratio.

### 3.3 Periodic array

This is the representation of an infinite number of repairs in the X direction, as shown in Fig. 8, and is equivalent to the tandem configuration. The height of the sheet is very large in comparison to the radius, and hence can be assumed to be infinite. The loading is carried out by applying uniform displacements in the X direction along the face of the sheet. This results in a variation of  $\sigma_x$  stress in the Y direction and from this an average stress has been calculated. Results for a range of  $E_o / E_s$  are presented in Fig. 9 and correspond to point A shown in Fig. 8. Although the separation distance is considered in terms of  $W/R$  ratio's, it is apparent that at close separations maximum stress ratio's of 1.9 are achieved at point A, with a value of  $E_o / E_s = 3.0$ . However for most repairs the maximum stress ratio would be 1.55.

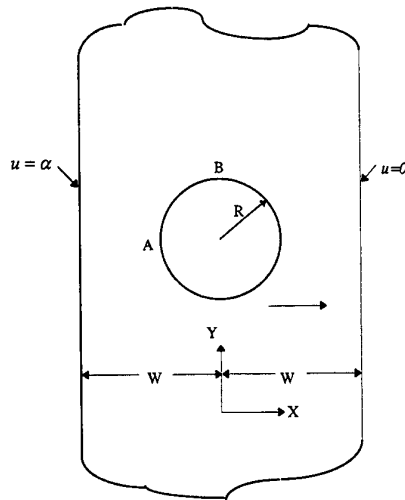


Figure 8. Periodic array in  $x$  direction (tandem configuration), infinite in  $y$  direction.

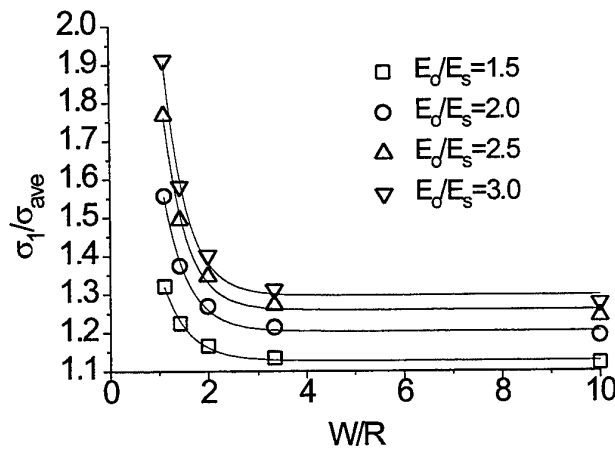


Figure 9. Results for periodic array, stress ratio  $\sigma_1/\sigma_{ave}$  for  $W/R$  ratios.

### 3.4 Combination of loads

A bi-axial stress field has been considered in which the applied stresses are  $\sigma_x = 1$  and  $\sigma_y = -1$ , corresponding to the geometry in Fig. 2. These results are shown in Fig. 10. In this case the maximum interaction occurs at location C (see Fig. 2) corresponding to the lower  $S/R$  ratios. Again the repairs with large  $E_o/E_s$  ratios result in the largest  $\sigma_1/\sigma_x$  ratios. The maximum principal stress also happens to occur in the  $X$  direction. This combination of loads results in a stress interaction equal to that of the periodic array. For the case where  $\sigma_x = \sigma_y = 1$ , for the geometry shown in Fig. 2, results obtained are shown in Fig. 11. In comparison to Fig. 5 for the uni-axial case, the combination of stresses alleviates the interaction effect. Clearly, the direction of the load components is important.

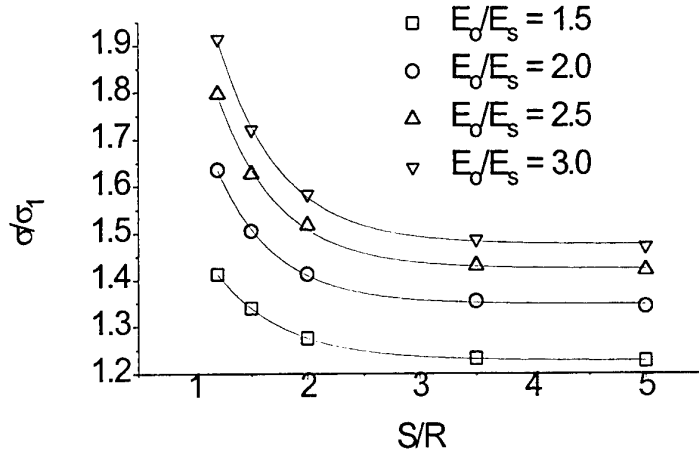


Figure 10. Bi-axial loading:  $S/R=1.1$ ,  $\sigma_x = 1$ ,  $\sigma_y = -1$ , stress ratio at point C.

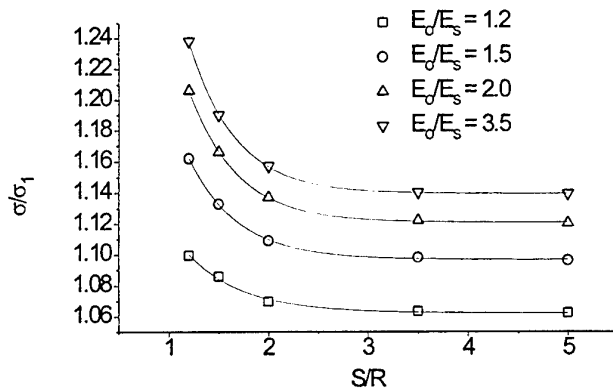


Figure 11. Bi-axial loading,  $S/R=1.1$ ,  $\sigma_x = 1$ ,  $\sigma_y = 1$ , stress ratio at point C.

### 3.5 Finite width effect

Consider the tandem configuration shown in Fig. 12. In this case the  $S/R$  ratio has been set to 1.1 since it is already known that the highest interaction occurs with this geometry. The results shown in Fig. 13 show a percentage change of sheet stress (location C) with a variation of width,  $W$ , (expressed as a ratio  $W/R$ ). The greatest reduction in sheet stress occurs for  $W/R$  ratios approaching 1, and for higher  $E_o/E_s$  ratios.

For the case of the side by side configuration shown in Fig. 14 the S/R ratio adopted was 3 since the highest stress occurs at large separations. The results for the percentage change of sheet stress (location B) versus W/R are shown in Fig. 15. Again the largest reductions of sheet stress occur for W/R ratios approaching 1, and for higher  $E_o / E_s$  ratios. In comparison with the tandem configuration the finite width effect is not as strong. The results may be surprising that a smaller width should decrease the sheet stress, but an explanation is that with a narrow width the load attraction ability is limited.

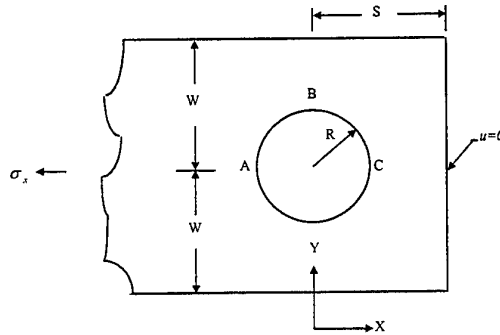


Figure 12. Finite width effect: tandem configuration.

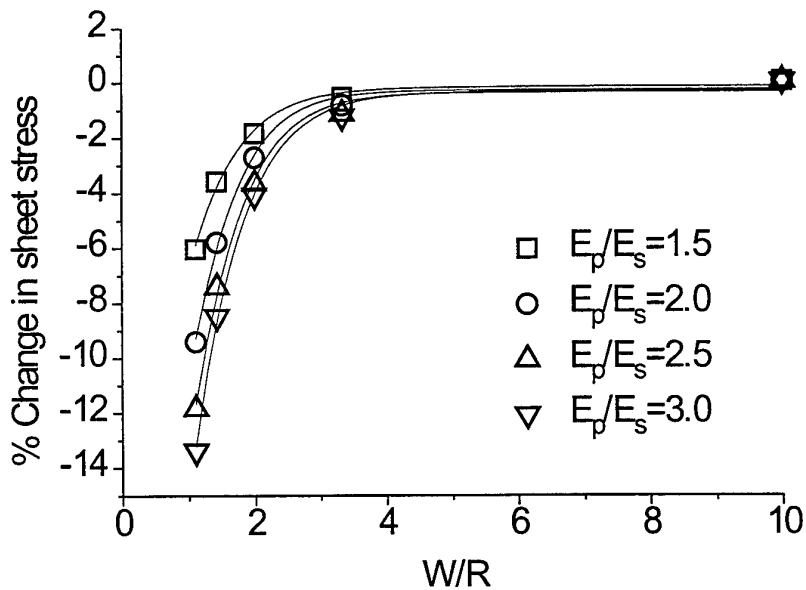


Figure 13. Finite width effect: % Change in sheet stress for tandem configuration.

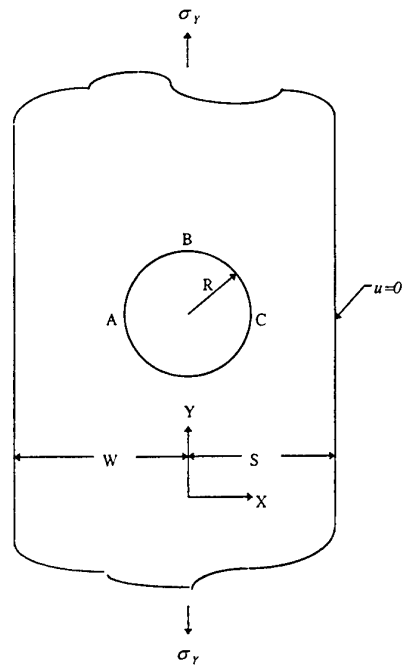


Figure 14. Finite width effect: side by side configuration.

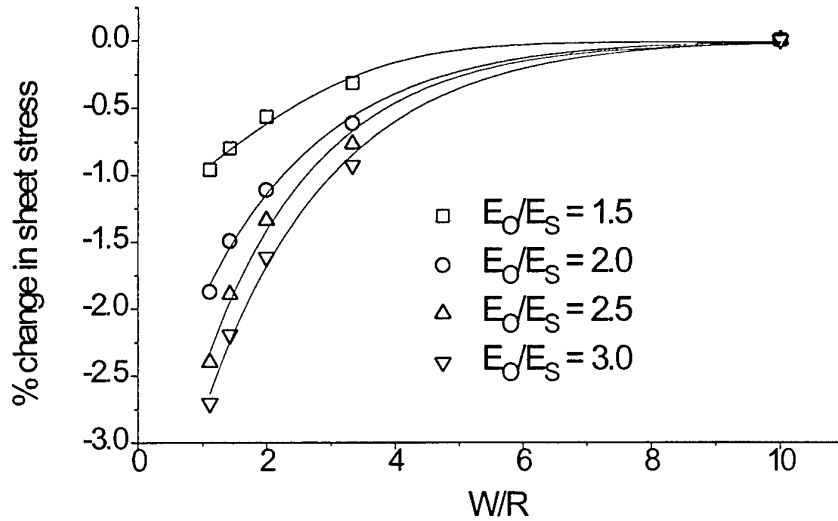


Figure 15. Finite width: % Change in sheet stress for side by side configuration.

## 4. Validation

The purpose of the validation is to verify the accuracy to which stresses can be predicted just outside a repair for a given mesh density. In particular, the mesh density used in the interaction study. Consider a circular repair on a circular 2D sheet as shown in Fig. 16. The sheet is subject to a uniform pressure load applied to the perimeter of the sheet in a radial direction. The patch region has a radius  $r=R_I$ , while the radius of the circular sheet is  $r=R_O$ . Quantities  $R_I$ ,  $E_O, t_O, u_O$  and  $\sigma_O$  are relevant to the patch region for  $r \leq R_O$ , while quantities  $R_O$ ,  $E_S, t_S, u_S$  and  $\sigma_S$  correspond to the sheet region where  $R_I \leq r \leq R_O$ .

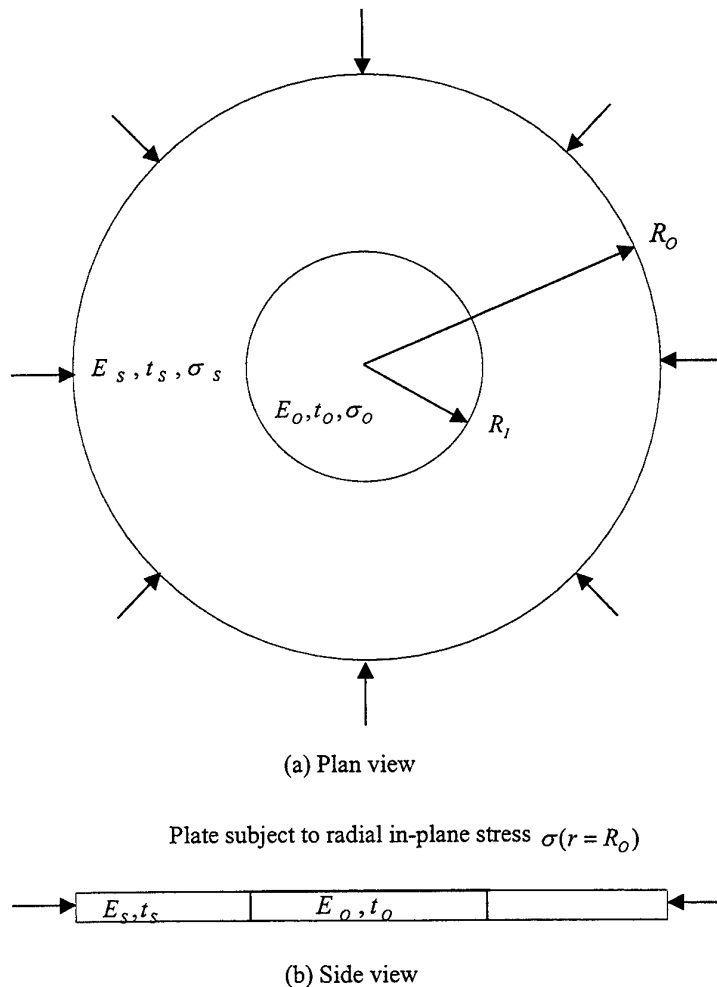


Figure 16. Variables for closed form solution for a circular repair on a circular sheet.

Firstly the radial stresses and displacements will be obtained for the sheet and patch. Consider the configuration with properties as shown in Fig. 16. The governing equation is given by Timoshenko & Goodier [6] as:

$$\frac{d^2u}{dr^2} + \frac{1}{r} \frac{du}{dr} - \frac{u}{r^2} = 0 \quad (2)$$

where  $u$  is the radial displacement  
 $r$  is the radial distance

The solution of this equation is given by:

for  $r \geq R_I$

$$u_1 = C_2 r + \frac{C_3}{r} \quad (3)$$

for  $r \leq R_I$

$$u_o = C_1 r \quad (4)$$

where  $C_1$ ,  $C_2$  and  $C_3$  are constants of integration.

It can also be shown from [6] that the radial stress is given by:

for  $r \geq R_I$

$$\sigma_s = \frac{E_s}{(1-\nu^2)} \left[ C_2(1+\nu) - \frac{C_3(1-\nu)}{r^2} \right] \quad (5)$$

for  $r \leq R_I$

$$\sigma_o = \frac{E_o}{(1-\nu^2)} C_1(1+\nu) \quad (6)$$

It is now necessary to solve for the three constants of integration. The solution of these equations must satisfy the following conditions:

(a) The displacement  $u_s$  and  $u_o$  is equal at  $r = R_I$ , hence from equations (3) and (4):

$$C_2 r + \frac{C_3}{r} = C_1 R_I \quad (7)$$

(b) Equilibrium must be maintained across the boundary at  $r = R_I$  (note that  $t_s = t_o$ ), using equations (5) and (6) leads to:

$$\frac{E_s t_s}{(1-\nu^2)} \left[ C_2(1+\nu) - \frac{C_3(1-\nu)}{R_I^2} \right] = \frac{E_o t_o}{(1-\nu)} C_1 \quad (8)$$

(c) Also we have the from equ(6) that at  $r \leq R_I$ :

$$\sigma_o = \frac{E_o}{(1-\nu^2)} C_1(1+\nu) \quad (9)$$

At this stage we have enough information for the evaluation of the constants  $C_1$ ,  $C_2$  and  $C_3$ , hence:

$$C_1 = \frac{(1-\nu)}{E_o} \sigma_o \quad (10)$$

$$C_2 = (1-\nu) \sigma_o \left[ \frac{1}{E_o} - \frac{(1+\nu)}{2} \left( \frac{1}{E_o} - \frac{1}{E_1} \right) \right] \quad (11)$$

$$C_3 = \frac{R_I^2}{2} (1-\nu^2) \sigma_o \left[ \frac{1}{E_o} - \frac{1}{E_s} \right] \quad (12)$$

Using equ(5, 6) for  $\sigma_1$  and  $\sigma_o$  we obtain the following:

$$\frac{\sigma_s}{\sigma_o} = \left\{ \frac{E_s}{E_o} + 0.5 \left( 1 - \frac{E_s}{E_o} \right) \left[ (1+\nu) + \left( \frac{R_I}{r} \right)^2 (1-\nu) \right] \right\} \quad (13)$$

Results for two  $E_s / E_o$  ratios are shown in Fig. 18 together with the F.E. results. The F.E. mesh is shown in Fig. 17. Very good agreement between the closed form solution and F.E. results has been achieved. It is evident that the stress, just outside the patch, can be predicted to a high degree of accuracy. Since a similiar radial mesh density has been used in the interaction study, this gives confidence in the results that have been obtained in the repair interaction.

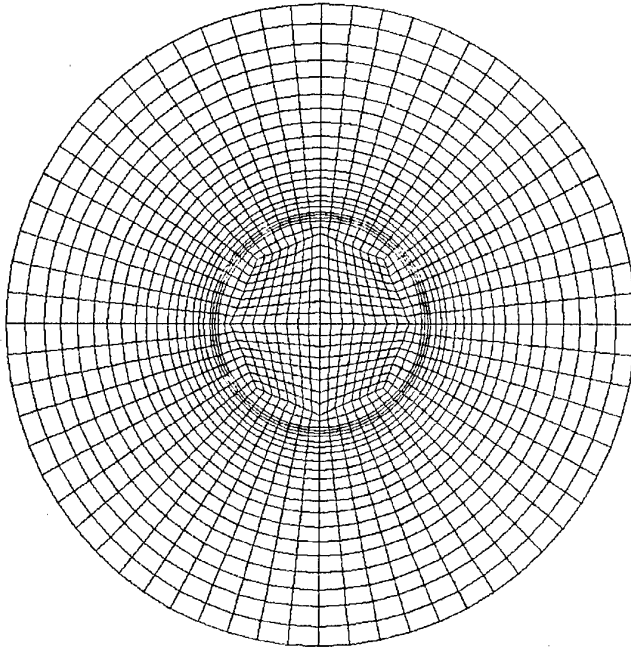


Figure 17. F.E. mesh for validation of circular repair on a circular plate,  $R_i=162$ .mm,  $R_o=500$ .mm.

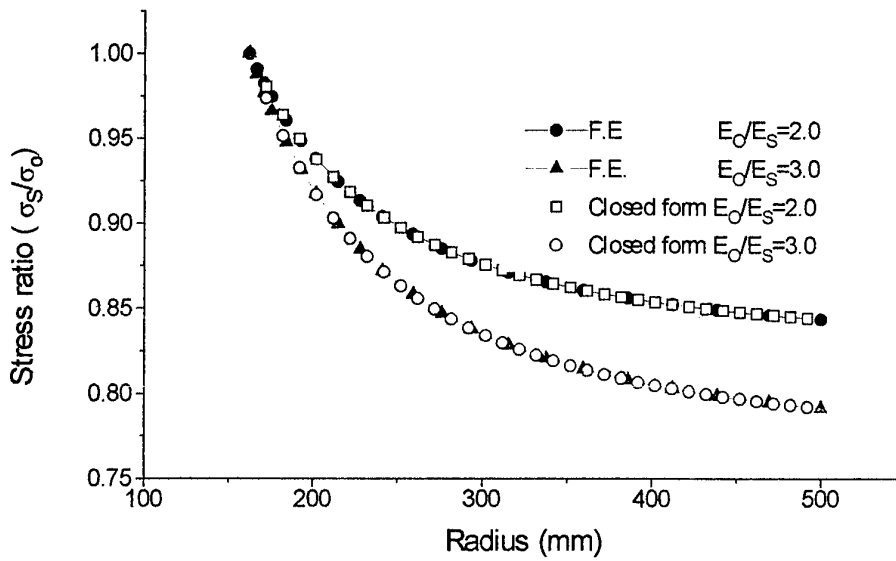


Figure 18. Validation of F.E. work using closed form solution for a single repair.

## 5. Conclusion

Firstly, the validation using a closed form solution for a single repair, also derived here, gives very good agreement with the F.E. results. This gives confidence that the stress predictions in the sheet, just outside interacting repairs, is accurate. Results for the repair interaction indicate that maximum stress increases, depend on both the orientation of the repair with respect to the applied load, and separation distance between repairs. The side by side configuration with respect to the applied load gave stress increases of between 12-27%, where the maximum values occurred at the larger separation distances. In the case of the tandem configuration with respect to the applied load, stress increases of between 23-60% were obtained and the maximum correspond to small separation distances. In both orientations over stiff repairs gave the maximum stress increases. Thus, shielding and load-shedding behaviour for neighbouring repairs is in complete contrast to that for neighbouring holes or cutouts, which could be regarded as limiting cases for which  $E_o/E_s \rightarrow 0$ , whereas for repairs  $E_o/E_s > 1$ .

Bi-axial loading combinations can either increase or decrease the stress field interactions. If the applied component stresses are of the same sign interaction stresses are decreased; while applied stresses of opposite signs result in increased interaction stresses. Results from the study of the periodic array in one direction have shown that this configuration gives the highest stress increases for uni-axial loading, and also is a tandem orientation with respect to the load. Furthermore it has been shown that the location of the maximum stresses are independent of the S/R ratio. An investigation of the finite width effect has shown that repairs in sheets with small widths result in smaller stresses than in large width sheets. In this case the repair is no longer able to attract additional load from the surrounding structure.

The design of bonded repair procedures is well documented in the RAAF Engineering Standard C5033. However the current load attraction factor used is independent of the separation distance between repairs. The design curves presented here, when used together with material S-n data, will enable the RAAF to more accurately assess the fatigue life of the sheet just outside repairs.

## 6. Acknowledgment

The authors wish to acknowledge Dr M.Heller for assistance in the preparation of this report.

## 7. References

1. W.T.Chow and S.N.Atluri. Composite patch repairs of metal structures - Adhesive non-linearity. AIAA Journal, vol.35, no. 9, Sept 1997.
2. Anon. RAAF Engineering Standard C5033. Composite Materials and Adhesive Bonded Repairs.
3. L.R.F.Rose. Theoretical Analysis of Crack Patching, in Bonded Repair of Aircraft Structures, A.A. Baker and R. Jones (eds.), Martinus Nijhoff (1988).
4. L.R.F.Rose, R.J.Callinan, A.A.Baker, S.Sanderson and E.S.Wilson. Design Validation for a Bonded Composite Repair to the F-111 Lower Skin. PICAST-AAC6 Conference, Melbourne, March 20-23, 1995.
5. C.H.Wang, L.R.F.Rose and R.J.Callinan. Analysis of out-of-plane bending in one-sided bonded repair. Int. J. Solids Structures Vol. 35, No. 14, pp. 1653-1675, 1998.
6. S.P.Timoshenko and J.N.Goodier. Theory of Elasticity. Third edition, McGraw-Hill Book Company, 1970.

## DISTRIBUTION LIST

Analysis of the Interaction Effect for Bonded Repairs

R.J.Callinan, L.R.F.Rose and S.Sanderson

### AUSTRALIA

#### DEFENCE ORGANISATION

**Task Sponsor**            **AIROIC-ASI-LSA**

#### **S&T Program**

Chief Defence Scientist  
FAS Science Policy  
AS Science Corporate Management  
Director General Science Policy Development  
Counsellor Defence Science, London (Doc Data Sheet )  
Counsellor Defence Science, Washington (Doc Data Sheet )  
Scientific Adviser to MRDC Thailand (Doc Data Sheet )  
Director General Scientific Advisers and Trials/Scientific Adviser Policy and  
    Command (shared copy)  
Navy Scientific Adviser (Doc Data Sheet and distribution list only)  
Scientific Adviser - Army (Doc Data Sheet and distribution list only)  
Air Force Scientific Adviser  
Director Trials

} shared copy

#### **Aeronautical and Maritime Research Laboratory**

Director

Chief of Airframes and Engines Division  
Research Leader: Dr L.R.F.Rose  
Task Manager: Dr M.Heller  
R.J.Callinan  
S.Sanderson

#### **DSTO Library**

Library Fishermens Bend  
Library Maribyrnong  
Library Salisbury (2 copies)  
Australian Archives  
Library, MOD, Pymont (Doc Data sheet only)

#### **Capability Development Division**

Director General Maritime Development (Doc Data Sheet only)  
Director General Land Development (Doc Data Sheet only)  
Director General C3I Development (Doc Data Sheet only)

## **Army**

ABCA Office, G-1-34, Russell Offices, Canberra (4 copies)  
SO (Science), DJFHQ(L), MILPO Enoggera, Queensland 4051 (Doc Data Sheet only)  
NAPOC QWG Engineer NBCD c/- DENGRS-A, HQ Engineer Centre Liverpool Military Area, NSW 2174 (Doc Data Sheet only)

## **Intelligence Program**

DGSTA Defence Intelligence Organisation

## **Corporate Support Program (libraries)**

OIC TRS, Defence Regional Library, Canberra  
Officer in Charge, Document Exchange Centre (DEC) (Doc Data Sheet and distribution list only)  
\*US Defence Technical Information Center, 2 copies  
\*UK Defence Research Information Centre, 2 copies  
\*Canada Defence Scientific Information Service, 1 copy  
\*NZ Defence Information Centre, 1 copy  
National Library of Australia, 1 copy

## **UNIVERSITIES AND COLLEGES**

Australian Defence Force Academy  
Library  
Head of Aerospace and Mechanical Engineering  
Deakin University, Serials Section (M list), Deakin University Library, Geelong,  
Senior Librarian, Hargrave Library, Monash University  
Librarian, Flinders University

## **OTHER ORGANISATIONS**

NASA (Canberra)  
AGPS

## **OUTSIDE AUSTRALIA**

### **ABSTRACTING AND INFORMATION ORGANISATIONS**

INSPEC: Acquisitions Section Institution of Electrical Engineers  
Library, Chemical Abstracts Reference Service  
Engineering Societies Library, US  
Materials Information, Cambridge Scientific Abstracts, US  
Documents Librarian, The Center for Research Libraries, US

### **INFORMATION EXCHANGE AGREEMENT PARTNERS**

Acquisitions Unit, Science Reference and Information Service, UK  
Library - Exchange Desk, National Institute of Standards and Technology, US

SPARES (5 copies)

**Total number of copies: 46**

<b>DEFENCE SCIENCE AND TECHNOLOGY ORGANISATION DOCUMENT CONTROL DATA</b>		1. PRIVACY MARKING/CAVEAT (OF DOCUMENT)			
		2. TITLE  Analysis of the Interaction Effect for Bonded Repairs		3. SECURITY CLASSIFICATION (FOR UNCLASSIFIED REPORTS THAT ARE LIMITED RELEASE USE (L) NEXT TO DOCUMENT CLASSIFICATION)  Document (U) Title (U) Abstract (U)	
4. AUTHOR(S)  R.J. Callinan, L.R.F. Rose and S. Sanderson		5. CORPORATE AUTHOR  Aeronautical and Maritime Research Laboratory PO Box 4331 Melbourne Vic 3001			
6a. DSTO NUMBER DSTO-TR-0715	6b. AR NUMBER AR-010-621	6c. TYPE OF REPORT Technical Report	7. DOCUMENT DATE August 1998		
8. FILE NUMBER M1/9/353	9. TASK NUMBER 95/228	10. TASK SPONSOR AIROIC-ASI-LSA	11. NO. OF PAGES 18	12. NO. OF REFERENCES 6	
13. DOWNGRADING/DELIMITING INSTRUCTIONS		14. RELEASE AUTHORITY  Chief, Airframes and Engines Division			
15. SECONDARY RELEASE STATEMENT OF THIS DOCUMENT  <i>Approved for public release</i>					
OVERSEAS ENQUIRIES OUTSIDE STATED LIMITATIONS SHOULD BE REFERRED THROUGH DOCUMENT EXCHANGE CENTRE, DIS NETWORK OFFICE, DEPT OF DEFENCE, CAMPBELL PARK OFFICES, CANBERRA ACT 2600					
16. DELIBERATE ANNOUNCEMENT  No Limitations					
17. CASUAL ANNOUNCEMENT		Yes			
18. DEFTEST DESCRIPTORS  Finite element analysis, Bonded composite repairs, Interactions					
19. ABSTRACT  With the increasing use of bonded repairs to restore the structural integrity of ageing aircraft the question arises as to the interaction effects when repairs are located close together. Using the Finite Element (F.E.) method a study has been carried out for the interaction between two idealised circular repairs. The interaction involves the increase of the sheet stress just outside the patch. It has been found that the tandem orientation, with respect to the applied load, is the most severe configuration. In this case, for most practical repairs, the interaction may result in increases of the sheet stress by 40% for very close separation distances. It has also been found that certain combinations of bi-axial load can also significantly influence the interaction effect.					